Macromolecular Bioscience
www.mbs-journal.de

Emulsion Techniques for the Production of Pharmacological Nanoparticles

*Ratchapol Jenjob, Treethip Phakkeeree, Farzad Seidi, Man Theerasilp, and Daniel Crespy**

Nanoparticles have the advantages over micron-sized particles to typically provide higher intracellular uptake and drug bioavailability. Emulsion techniques are commonly used methods for producing nanoparticles aiming at high encapsulation efficiency, high stability, and low toxicity. Here, the recent developments of nanoparticles prepared from emulsions, the synthesis of nanoparticles, their physicochemical properties, and their biomedical applications are discussed. Selection of techniques, such as emulsion polymerization, miniemulsion polymerization, microemulsion polymerization, and emulsion-solvent evaporation processes, strongly influences morphologies, size distributions, and particle properties. Details in the synthetic strategies governing the performance of nanoparticles in bioimaging, biosensing, and drug delivery are presented. Benefits and limitations of molecular imaging techniques are also discussed.

1. Introduction

With the advent of nanomedicine, the preparation of nanoparticles for pharmaceutical applications has been widely applied for medical diagnostics and drug delivery.[1–5] Nanoparticles can be prepared by a wide variety of chemical or physical methods. Spray drying is a physical process that is relevant for industrial applications used for the production of microparticles. Nowadays, spray drying have been further developed to allow for producing smaller particles with a size range between 100 nm to 5 microns.[6] Particles are formed by atomizing an emulsion into a stream of hot air under vigorous solvent evaporation. Electrospray is a flow of constant liquid and pressure typically pressed through a needle subjected to high electrical field. Fine droplets are produced and the solvent is evaporated during their move toward the collector.[7] This process is largely influenced and controlled by liquid viscosity, needle diameter, pressure, and distance between needle tip and collector plate. Moreover, polymer concentration is also crucial because too large concentrations may produce fibers (electrospinning).[8] Additionally, electrospray can be used to fabricate nanoparticles with more narrow size distribution than nanoparticles produced by spray drying. For these two processes, the polymers are prepared before formation of nanoparticles. Therefore, the chemical structure, morphology of nanoparticles, and functionality are typically less complex than what can be produced from emulsion techniques.

Emulsions are mixtures of two or more immiscible liquids in which one or more liquids are dispersed in another liquid. Emulsions such as water-in-oil (W/O), oil-in-water (O/W), oil-in-water-in-oil (O/W/O), or water-in-oil-in-water (W/O/W) are commonly used for pharmacological applications (**Figure 1**).[9] Emulsions are usually thermodynamically unstable and coalescence of droplets occurs to minimize the Gibbs free energy of the system.[10] Therefore, surfactants and stabilizers are necessary to stabilize emulsion droplets. Some processes provide very high encapsulation efficiency of payloads, especially double/multiple emulsion or miniemulsion techniques.[11] As a typical example, essential oils could be encapsulated in silica nanocapsules prepared by the miniemulsion process with more than 90% encapsulation efficiency.[12] We describe here emulsion methods to create pharmacological nanoparticles with different structures and particle diameters. Then, we discuss their applications for pharmaceutical applications and discuss advantages and limitations of each molecular imaging technique for bioimaging applications.

2. Techniques to Produce Pharmacological Nanoparticles

2.1. Emulsion Polymerization

Heterophase polymerization processes are the most common and industrially used techniques to produce polymer nanoparticles.[13,14] Among them, emulsion polymerization is the major heterogeneous polymerization process. In a direct process, that is, in oil-in-water emulsions, hydrophobic monomers are emulsified in an aqueous continuous phase, followed by polymerization.[15,16] Surfactants, providing electrostatic, steric, or electrosteric stabilization, are typically required to stabilize the colloidal system and avoid coagulation during polymerization.[17] Emulsion polymerization provides submicron polymer particles, typically with an average size between 50 and 500 nm.[18] A typical particle contains 1 to 10 000 macromolecules, and each macromolecule is composed

Dr. R. Jenjob, Dr. T. Phakkeeree, Dr. F. Seidi, Dr. M. Theerasilp, Prof. D. Crespy
Department of Materials Science and Engineering
School of Molecular Science and Engineering
Vidyasirimedhi Institute of Science and Technology (VISTEC)
Rayong 21210, Thailand
E-mail: daniel.crespy@vistec.ac.th

The ORCID identification number(s) for the author(s) of this article can be found under https://doi.org/10.1002/mabi.201900063.

DOI: 10.1002/mabi.201900063

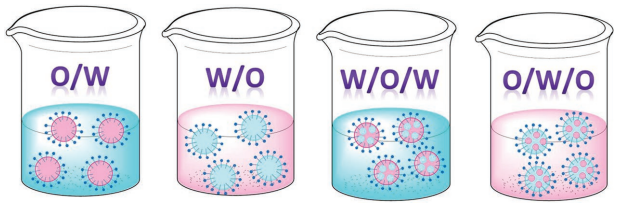

Figure 1. Type of emulsions: oil-in-water (O/W), water-in-oil (W/O), water-in-oil-in-water (W/O/W), and oil-in-water-in-oil (O/W/O) emulsions.

of about 100 to 106 monomer units.[19] In inverse emulsion polymerization, hydrophilic monomers such as acrylamide, acrylic acid, or methacrylic acid are emulsified in a continuous phase and polymerized.[20]

A cornucopia of reports describes the use of emulsion polymerization techniques describing the fabrication of nanoparticles for biomedical applications. Zhao et al. studied the photoluminescence of pH- and thermo-sensitive polystyrene-poly(*N*-isopropylacrylamide) (PS-PNIPAM)/poly(*N*-isopropylacrylamide)-poly(acrylic acid) (PNIPAM-PAA) core–shell particles as bioprobes (**Figure 2**A).[21] These core–shell particles displayed different emission colors upon excitation by a single wavelength to distinguish cancer cells from healthy cells. Core–shell magnetic particles for magnetic resonance imaging (MRI) and optical imaging (OI) were also prepared by emulsifier-free emulsion polymerization.[22] The prepared particles were composed of a core containing oleic acid (OA) and sodium undecylenate (NaUA)-modified Fe_3O_4 nanoparticles. The shell contained styrene, glycidyl methacrylate (GMA), and polymerizable gadolinium and europium complexes. The hydrodynamic diameter of these magnetic core–shell particles was 110–170 nm.

Additionally, emulsions can be stabilized by solid particles from Pickering emulsions.[23] Pickering emulsions are emulsion of particle-stabilized emulsions (O/W, W/O, or multiple emulsions) characterized by long-term stability. In recent years, colloidal particle–stabilized Pickering emulsions have attracted considerable interest due to their superior stability against coalescence. Yang et al. reviewed the use of various solid particles such as silica, clay, magnetic nanoparticles, and nanotubes as Pickering emulsifiers as well as their applications in different fields.[24] Pickering emulsions can be used in a wide range of applications such as cosmetics, biomedicine, and food science. Sun et al. used bovine hemoglobin (BHb)-coated Janus hydroxyapatite nanoparticles (BCJHP) for stabilizing Pickering emulsions.[25] Janus hydroxyapatite nanoparticles possessing both hydrophobic and hydrophilic parts were synthesized by partial masking with ultrapure water, and their remaining external part was modified with hydrophobic *n*-octadecyltrimethoxysilane, as well as further coating with BHb. Then, the obtained BHb-coated Janus nanoparticles were used as Pickering stabilizers for the emulsion polymerization of 2,2-bis(hydroxymethyl)propionic acid and 2-acrylamide-2-methylpropanesulfonic acid. The authors also proposed that adjusting the charged monomer composition modulated the rebinding capacity and specificity of imprinted polymers towards BHb. Starch is an abundant and cheap natural polysaccharide that has been widely studied for biomedical applications. Therefore, starch nanoparticles were used as stabilizers for the Pickering polymerization of styrene.[26]

Ratchapol Jenjob studied chemistry and continued with a Ph.D. in polymer science and technology at Mahidol University, Thailand. After Ph.D. graduation in 2012, he moved to South Korea to work at Utah-Inha DDS & Advanced Therapeutics Research Center as a postdoctoral fellow. In 2014–2015, he joined Dr. Su-Geun Yang's group at School of Medicine, Inha University Hospital, South Korea. He is now working as a group leader in the laboratory of Prof. Crespy at the Vidyasirimedhi Institute of Science and Technology (VISTEC). His expertise is the design and synthesis of nanoparticles/microparticles for various applications.

Treethip Phakkeeree received her Ph.D. from Kyoto Institute of Technology, Japan, in 2017. She subsequently became a project assistant professor at the Research Strategy Promotion Center at Kyoto Institute of Technology for 6 months. Now, she is a postdoctoral researcher at the COOL laboratory at Vidyasirimedhi Institute of Science and Technology (VISTEC), Thailand, to continue her research with new exciting aspects on polyurethane, anticorrosion, and drug delivery.

Daniel Crespy studied chemistry at the University of Strasbourg, France, and completed his Ph.D. under the supervision of Prof. Katharina Landfester at the University of Ulm, Germany. In 2006, he held a position as project leader at Empa (Swiss Federal laboratories for Materials Research and Technology). He joined the department of Prof. K. Landfester in July 2009 as group leader. Daniel Crespy is now associate professor at the Vidyasirimedhi Institute of Science and Technology (VISTEC) in Rayong, Thailand.

Amphiphilic starch-based nanoparticles were synthesized from starch octenyl succinic ester via a nano-coprecipitation process. Before polymerization of styrene, the starch nanoparticles were labeled with FITC in order to observe their distribution in styrene droplets. Styrene emulsion droplets were densely surrounded by FITC-labeled starch nanoparticles. Moreover,

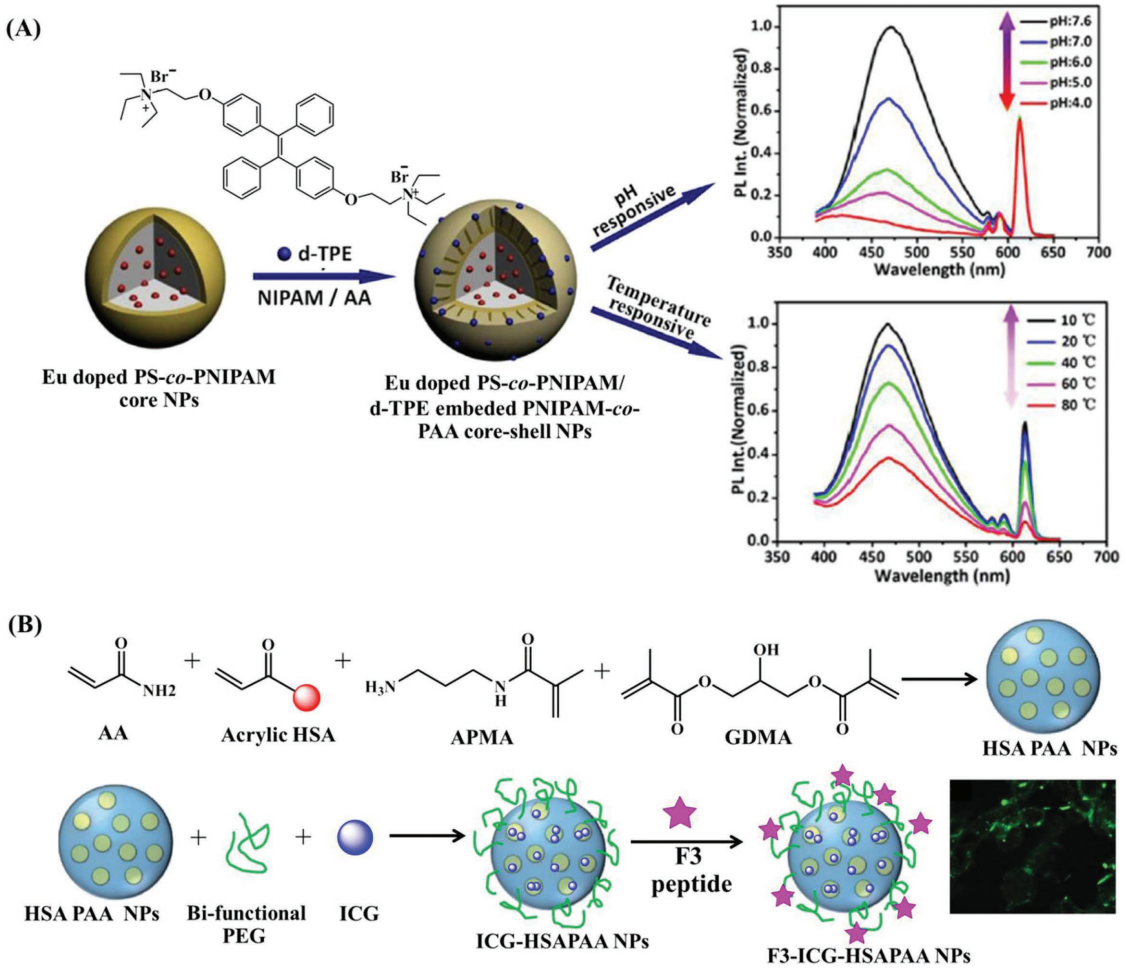

Figure 2. A) Schematic illustration of the synthetic process of the temperature- and pH-response with dual emission of Eu-doped PS-*co*-PNIPAM/d-TPE-embedded PNIPAM-*co*-PAA core/shell nanoparticles. The Eu-doped PS-*co*-PNIPAM core was prepared by a surfactant-free emulsion polymerization system. The core/shell nanoparticles Eu-doped PS-*co*-PNIPAM/PNIPAM-*co*-PAA were synthesized through a seed emulsion polymerization. A red-emission rare-earth complex and a blue-emission quaternary ammonium tetraphenylethylene derivative (d-TPE) with similar excitation wavelengths were inserted into the core and shell of the hydrogel nanoparticles, respectively. The PL intensities of the nanoparticles exhibited a linear temperature response in the range from 10 to 80 °C. Blue emission from the shell exhibited a linear pH response between pH 6.5 and 7.6. Reprinted with permission.[21] Copyright 2016, American Chemical Society. B) Modified human serum albumin (HSA) was first added into a mixture of acrylamide (AA), *N*-(3-aminopropyl) methacrylamide hydrochloride (APMA), and glycerol dimeathacrylate (GDMA) under stirring. The obtained mixture was then added into deoxygenated hexane containing surfactants. After mixing, initiator was added to start polymerization and the final products were HSA-PAA nanoparticles. Bi-functional PEG and indocyanine green (ICG) were added into HSA-PAA nanoparticles. Confocal images of F3-targeted selective delivery of ICG. Modified with permission.[44] Copyright 2013, the Royal Society of Chemistry.

thermoresponsive core–shell nanoparticles of polystyrene/poly(*N*-isopropylacrylamide)-silica have been prepared by one-step Pickering emulsion polymerization with a nonionic initiator.[27] The cancer drug 17-(allylamino)-17-demethoxygeldanamycin (17-AAG) was incorporated into the core of the nanoparticles. Cellular uptake and cytotoxicity were studied in prostate cancer (PC3) cells. Thermoresponsive nanoparticles loaded with 17-AAG–induced large dose-dependent death in PC3 cells at nanoparticle dosages from 0.01 to 1 μg mL^{-1}.

2.2. Miniemulsion Polymerization

Miniemulsion polymerization is a process for converting monomer droplets to polymer nanoparticles. Monomer droplets stabilized by surfactants are prepared by high shearing devices such as high-pressure homogenizer or ultrasonicator to yield stable and narrowly distributed droplets with a size ranging from 50 to 500 nm. The use of miniemulsion process for performing chain-growth polymerizations, polyadditions, polycondensations, and modifications of polymers was reviewed in another report.[28] Compared to other heterophase polymerizations, miniemulsion polymerization offers an incomparable flexibility to create polymeric nano-objects. Furthermore, miniemulsion droplets are stable against coalescence[29] and can be processed at high temperature.[30] Nanoparticle functionality can be tuned to offer responsive release of several payloads upon activation of external stimuli.[31] Miniemulsion droplets can be indeed used for ultrafast photopolymerization involving thiol–ene reactions.[32] Inverse miniemulsion polymerizations

refer to polymerization in polar droplets dispersed in apolar continuous media.[28,33] Inverse miniemulsion polymerization is an efficient process for encapsulating hydrophilic compounds such as DNA, RNA, proteins, and amino acids.

2.3. Microemulsion Polymerization

Microemulsions are thermodynamically stable dispersions of oil and water stabilized by surfactants and co-surfactants. Microemulsion droplet sizes are well below 100 nm.[34] Hou et al. designed the novel fluorescent microemulsion for delivery of nutraceuticals and active biological drugs using microemulsion method.[35] Microemulsion was prepared with isoamyl acetate (oil phase), polyoxyehtylene castor oil EL (CrEL) (surfactant), and water. The prepared microemulsions could emit bright blue fluorescence due to aromatic ring structure of polyoxyethylene ether substituent of CrEL in hydrophobic components, suggesting the potential for active drug detection for biosensor applications.

In direct microemulsion (oil-in-water, O/W) polymerizations, oil is replaced by a hydrophobic monomer and nanoparticles can be obtained after polymerization.[36] Microemulsion polymerization offers the advantage to yield stable dispersions with particle diameter typically 10–100 nm and a low polydispersity in size. However, microemulsion polymerization requires high surfactant concentration (≈10–15 wt%) relative to monomer (≈5 wt%) to form stable polymer particles.[37,38] The low polymer/surfactant ratio is an obvious drawback compared to conventional emulsion polymerizations, especially for biomedical applications.[36] High surfactant level can indeed influence the toxicity on cells and tissues.[39,40] Consequently, many efforts have been undertaken to obtain higher polymer content with lower surfactant concentration. Recently, Ming et al. developed a modified microemulsion polymerization by adding small amount of monomers into a reactor at the beginning of the reaction. Then, the remaining monomers were added dropwise to the prepolymerized microemulsion.[41] This method yielded polymer nanoparticles with an average diameter of 33–46 nm and a polymer content of 6–24 wt% with low surfactant concentration. In 2010, Chen and co-workers also developed a new method of microemulsion polymerization for synthesizing nanosized PMMA nanoparticles with ultrafine size distribution and minimization of surfactant content.[36] This new strategy involved monomer feeding system in which monomers were transferred as gas phase. The weight ratio of SDS/MMA was 1:20 (≈5 wt% of SDS in monomer phase), that is, much lower than other previous reports.[42,43] Since methyl methacrylate (MMA) monomers were fed uniformly in the gas phase, the PMMA nanoparticles (≈20 nm) can be prepared at much lower surfactant content compared with conventional methods. Yoon et al. encapsulated indocyanine green (ICG) as optical contrast agent in polyacrylamide–human serum albumin nanoparticles (HSA-PAA NPs).[44] The HSA-PAA NPs was synthesized from inverse microemulsion polymerization (water-in-oil). After loading of ICG into the HSA phase of the HSA-PAA nanoparticles, the targeting moiety, F3-Cys peptide, was attached on the surface of these nanoparticles for selective delivery to cancer cells, as shown in Figure 2B. The HSA-PAA nanoparticles loaded with ICG demonstrated high tumor cell selectivity and strong acoustic spectrum at 720 and 790 nm in the NIR range.

2.4. Emulsion-Solvent Evaporation Method

Emulsion-solvent evaporation method is popular because it is simple and provides nanoparticles that are prepared from purified polymers because emulsification occurs after the synthesis and purification of polymers.[45] Emulsion-solvent evaporation is a method for the emulsification of a dispersed phase containing polymers, solvents, and/or drugs in another phase (continuous phase), followed by evaporation of the solvents present in droplets. Typically, solution of polymers in low-boiling point solvents such as chloroform or dichloromethane are emulsified in water, followed by evaporation of the solvents to yield solid nanoparticles. However, polar polymer nanoparticles can be also prepared from inverse emulsions and subsequent evaporation of polar solvent such as hexafluoroisopropanol.[46] Subsequently, the nanoparticles are formed with sizes in the range of few hundred nanometers.[47] Guo et al. reported the encapsulation of anticancer compounds into PLGA nanoparticles by single emulsion-solvent evaporation.[48] Drug loading content and drug encapsulation efficiency were 7% and ≈58%, respectively. These carriers were used to improve photodynamic anticancer effect. However, sometimes emulsion-solvent evaporation has the limitation of low encapsulation efficiency of hydrophilic molecules because of rapid partitioning into the external aqueous phase when using single emulsion. Double emulsion-solvent evaporation method has potential for encapsulation of both hydrophilic and hydrophobic payloads with high encapsulation efficiency.[49] For instance, Liu et al. improved the encapsulation efficiency of daunorubicin (DNR) in PLGA nanoparticles using a double emulsion-solvent evaporation method.[50] Spherical PLGA nanoparticles displayed diameters of 200–300 nm with a remarkably high DNR encapsulation efficiency (>80%) and loading content (6.5%). Thermo- and pH-responsive polymeric nanocapsules for anticancer delivery were proposed by He and coworkers.[51] First, polyethylene glycol (PEG) and doxorubicin (DOX) solution (W1) were emulsified in dichloromethane (DCM) and acetone-containing copolymer of poly(*N*-isopropylacrylamide) and polyacrylic acid containing glycyrrhetinic acid (P(NIPAM-*co*-AAC-GA)) (O) by vortex to form W1/O emulsion. The primary emulsion was poured into polyvinyl alcohol (PVA) solution (W2) under stirring at fast rate to produce W1/O/W2 emulsions. The solvent was evaporated at room temperature. Resulting nanocapsules had a uniform size (approximately 450 nm) and hollow morphology with a loading efficiency up to 90%. Core–shell nanoparticles of gold nanoparticles (AuNPs) and nevirapine (NVP) prepared from double emulsion-solvent evaporation were developed by Dalvi and co-workers.[52] The designed core–shell nanoparticles were aimed at targeting delivery to multiple HIV reservoirs. AuNPs loaded with NVP exhibited particle diameter less than 250 nm and zeta potential −36 mV with high encapsulation efficiency (>70%) and loading content (≈40%). Moreover, Ahmed et al. demonstrated the synthesis of iron oxide/polycaprolactone particles as in vitro contrast agents for MRI.[53] Aqueous iron

oxide suspension was dispersed in DCM containing polycaprolactone using w/o emulsion method. The primary emulsion was transferred to PVA solution followed by evaporation of DCM. The prepared particles exhibited a nanosized range (250–350 nm) and superparamagnetic character.

3. Pharmacological Nanoparticles from Emulsion Techniques

Recently, the field of nanotechnology is gaining massive attention because nanoparticles can be fashioned with a wide range of materials that are suitable for specific applications, including bioimaging, biosensor, and drug delivery.[1] Moreover, nanoparticles are attractive in pharmaceutical applications because they contain large surface areas that can bind, adsorb, and carry the pharmaceutical compounds such as drugs, proteins, nucleic acids, vaccines, and probes.[54]

3.1. Pharmacological Nanoparticles for Bioimaging

Nanoparticles have been used in bioimaging as labels and contrast agents for a variety of molecular imaging techniques such as magnetic resonance imaging (MRI), positron emission tomography (PET), optical imaging (OI), computed tomography (CT), and ultrasound imaging (USI).[55] Each molecular imaging technique has certain advantages and limitations, as shown in **Table 1**.

Table 1. Advantages and disadvantages of various methods of molecular imaging.[56,57]

Molecular imaging technique	Advantages	Drawbacks
Optical imaging (OI)	1. High sensitivity 2. Low cost 3. No ionizing radiation	1. Limited penetration depth 2. Limited clinical translation
Magnetic resonance imaging (MRI)	1. High resolution 2. High soft tissue contrast 3. Clinical translation 4. No ionizing radiation 5. Non-invasiveness 6. Simultaneous acquisition of anatomical structure and physiological function	1. Expensive 2. Low sensitivity 3. Long imaging time
Positron emission tomography (PET)	1. High sensitivity 2. Clinical translation 3. Quantitative capability	1. Price 2. Radiation dose 3. Resolution 4. Long imaging time 5. Lack of parameter to identify molecular events with accurate correlation
Ultrasound imaging (USI)	1. Good temporal resolution 2. Quantitative data 3. Real time practice 4. Non-invasiveness 5. Low cost 6. No ionizing radiation	1. Only vascular contrast materials 2. Operator dependency
Computed tomography (CT)	1. High spatial resolution 2. Fast acquisition time 3. Relative simplicity 4. Excellent hard tissue imaging	1. Radiation dose 2. Ionizing radiation 3. Limited soft tissue contrast 4. Poor sensitivity

3.1.1. Optical Imaging

Optical molecular imaging is non-invasive and claimed to be safe. There are many optical imaging techniques that provide different penetration depths such as confocal, two-photon, tomography, fluorescence, polarization, or bioluminescence techniques.[58] Due to the advantages of OI such as high sensitivity and low price, OI was used to investigate tumor occurrence. However, since the energy of the photon is low, the depth of penetration into deep tissue in large subjects is limited. However, in the case of the small size of tissue, the depth of penetration can be tuned.[57] Furthermore, the penetration depth depends on the wavelength of light. For instance, the photons of UV–vis light are mostly absorbed by tissue chromophores such as deoxy- and oxyhemoglobin within few micrometers to millimeter of tissue thickness, resulting in a limitation of penetration depth. Andreas Reisch et al. have reviewed the strategies for the synthesis of dye-loaded polymer nanoparticles by emulsion polymerization, miniemulsion polymerization, microemulsion polymerization, and emulsion-solvent evaporation for in vitro and in vivo imaging.[59] The authors demonstrated the limitations of conventional dyes inside polymer nanoparticles and compared the concepts of dye design to reach high loading with reduced aggregation caused quenching. In emulsion polymerization approaches, the fluorescent dye is most often incorporated during the polymerization in the form of a dye monomer. Basically, polymerization takes place in the micelles (not in the initially dispersed monomer droplets). Thus, at high dye loading, both monomer and dye have to diffuse through the aqueous phase, which makes achieving a homogeneous dye loading more challenging. For miniemulsion and microemulsion polymerizations, dyes were encapsulated either through copolymerization,[60,61] physical encapsulation,[62] or after particle formation through swelling procedures.[63]

Recently, fluorescence resonance energy transfer (FRET) has been employed to design ratiometric sensor. These sensors are used for the quantitative analysis of biological events occurring under complex conditions, such as those inside cells by simultaneously recording fluorescence intensities at two wavelengths and calculating their ratios.[64] Chen et al. reported the synthesis of a lysosome-targetable ratiometric fluorescent nanoparticle as pH sensor.[65] 4-ethoxy-9-allyl-1,8-naphthalimide (EANI, donor) was copolymerized with MMA and 2-aminoethyl methacrylate hydrochloride (AEMH) by miniemulsion polymerization to obtain polymer nanoparticles. Fluorescein isothiocyanate (FITC, acceptor) was then conjugated on the polymer nanoparticles to produce pH-responsive FRET systems. FITC on the surface of the polymer nanoparticles displayed structural and spectral changes when pH changed. FRET occurred between the EANI (donor) in the particle cores and the surface acceptor (ring-opened FITC) when

the pH changed, achieving a ratiometric fluorescence recognition of pH in aqueous media. Selective accumulation of polymer nanoparticles in the lysosomes of living cells (HeLa cells) was observed. This system was then suitable to visualize intracellular lysosomal pH changes. The same group also synthesized reversibly photoswitchable fluorescent polymeric nanoparticles (PFPNs) with possible switching of emission between white light and any visible color in solution and films.[66] PFPNs were built up from three primary fluorescent dyes of (4-ethoxy-9-allyl-1,8-naphthalimide, 2-((7-nitrobenzo[c][1,2,5]oxadiazol-4-yl)amino) ethyl methacrylate, 9 (diethylamino)-5-oxo-5H-benzo-[a]phenoxazin-2-yl-methacrylate, and a photochromic diarylethene (DTE) molecule, by miniemulsion polymerization. The photochromic DTE derivative of (4,4′-(perfluorocyclopent-1-ene-1,2-diyl) bis(5-methylthiophene-4,2-diyl))bis-(methylene) diacrylate (DTEDA) was used to switch FRET process because it could undergo a reversible transition under light irradiation. The three dyes were encapsulated in cross-linked poly(methyl methacrylate) nanoparticles. By switching FRET from excited dyes to DTE moiety, these nanoparticles can switch between tricolored emission and complete quenching states. These PFPNs can be potentially used for bioimaging applications. High-contrast dual-color fluorescence imaging of living cells based on PFPNs was proposed by Jian et al.[67] Amphiphilic boron-dipyrromethene (BODIPY)-based PFPNs were synthesized by a facile one-pot RAFT-mediated miniemulsion polymerization of polymerizable BODIPY and spiropyran derivatives, together with MMA monomer and biocompatible PEO macro-RAFT agent. The amphiphilic BODIPY-based PFPNs showed reversibly photoswitchable fluorescence properties under the alternative UV and visible light illumination through induced intraparticle FRET (**Figure 3**A). The photoswitchable capability of PFPNs in living A549 (human lung carcinoma) cell lines was investigated under UV and visible light. Under visible light irradiation, the green fluorescence from cells was found because spiropyran-linked methacrylate (SPMA) moieties could not quench the fluorescence of BODIPY methacrylate (BDPMA). Consequently, the BDPMA in PFPNs emitted strong green fluorescence after excitation. After illuminating the cells with UV light, the green fluorescence from cells vanished whereas red fluorescence occurred. SPMA moieties in nanoparticles changed to ring-opened merocyanine (MC) state after irradiation of UV light and FRET process between MC state of SPMA and BDPMA occurred, leading to a dramatic quenching of the green fluorescence of BDPMA.

Fluorescence lifetime imaging microscopy (FLIM) has been widely used for biological research because it is a non-invasive imaging technique that can monitor the presence of fluorophores in cells or tissues by spatial variation of fluorescent lifetime.[68] Fluorescence lifetime is highly dependent on the local microenvironment of molecules but independent on dye concentration, photo-bleaching, and excitation intensity. Therefore, FLIM can indicate changes of microenvironment around drugs, reflecting intercellular drug release and transport inside the cells.[69] Zhou et al. used FLIM to monitor the dynamic change of DOX fluorescence lifetime in intercellular environments.[70] Poly(allylamine)-citraconic anhydride/doxorubicin (PAH-Cit/DOX) nanoparticles were prepared by emulsion solvent-evaporation and used as nanodrug system for the efficient delivery and pH-responsive release of DOX into cancer cells (MCF-7 cells). Once PAH-Cit/DOX nanoparticles were internalized into cancer cells, the DOX was released from the nanoparticles by acidic pH triggering in endosomes and lysosomes. DOX could then enter the nucleus to achieve its therapeutic effect. FLIM was used to monitor the release and subcellular distribution of DOX in cancer cells. FLIM analysis allowed for an optical separation of subcellular compartments such as cell membrane, cytoplasm, nucleus membrane, and nucleus, based on the difference of DOX fluorescence lifetime.

One important strategy for imaging deeper tissues is the use of near-infrared (NIR) light at 650–900 nm due to minimal absorption of tissues. Hence, near-infrared fluorescence (NIRF) imaging is mainly used in research with animals.[55] Yoon et al. encapsulated the indocyanine green (ICG) dye (optical contrast agent) in HSA-PAA nanoparticles presenting tumor targeting peptides on their surface.[44] At 3% of ICG loading, nanoparticles containing ICG showed the strongest fluorescence intensity and the photoacoustic spectrum of the NPs had two strong peaks in the NIR range. Thus, these nanoparticles were interesting for biomedical applications due to their strong fluorescence intensity and photoacoustic image (Figure 2B). The design of core–shell hydrogel particles of PS-PNIPAM/PNIPAM-PAA with dual photoluminescence for bioprobes was reported by Zhao and coworker.[21] A red emission rare-earth complex (Eu (III)) and a blue-emission quaternary ammonium tetraphenylethylene derivative (d-TPE) with similar excitation wavelengths were encapsulated in the core and shell of these hydrogel nanoparticles, respectively. The photoluminescence intensities of the nanoparticles displayed a linear temperature response in the range from 10 to 80 °C. The blue emission from the shell exhibited a linear pH response between pH 6.5 and 7.6, while the red emission from the core was pH-independent (Figure 2A). These stimuli-responsive core–shell nanoparticles have potential applications in bio- and chemosensors, biological imaging, cancer diagnosis, and for the externally activated release of anticancer drugs. Recently, efforts have been made to develop imaging-guided cancer therapy to enhance the therapeutic efficiency and minimize side effects. Photothermal imaging (PTI) in non-invasive mode offered better contrast of living cell image than conventional optical imaging.[71] PTI offers good temperature sensitivity and possibility of real-time monitoring. Unlike other optical imaging techniques, PTI does not require any fluorescent tags and thus can be ascribed as non-labeling technique. It is often applied in conjunction with photothermal therapy (PTT) and photodynamic therapy (PDT).[72] Under NIR irradiation, photosensitizers can generate high singlet oxygen quantum yield, showing photothermal conversion efficiency and outstanding photoacoustic response–guided simultaneous PDT and PTT. Zhou et al. reported the synthesis of polyaniline (PANI)-loaded γ-polyglutamic acid (γ-PGA) nanogels for photoacoustic imaging–guided PTT of tumors.[73] γ-PGA nanogels were first synthesized via a double emulsion-solvent evaporation process, followed by crosslinking with cystamine dihydrochloride. γ-PGA/Cys nanogels were then used as nanoreactors for polymerizing aniline. Theranostic potential of the γ-PGA/Cys@PANI nanogels was characterized by PTI in xenografted tumor model. Dynamic whole-body infrared thermal images of tumor-bearing mice after intratumoral injection of γ-PGA/Cys@PANI nanogels were collected by a photothermal medical device. This finding revealed

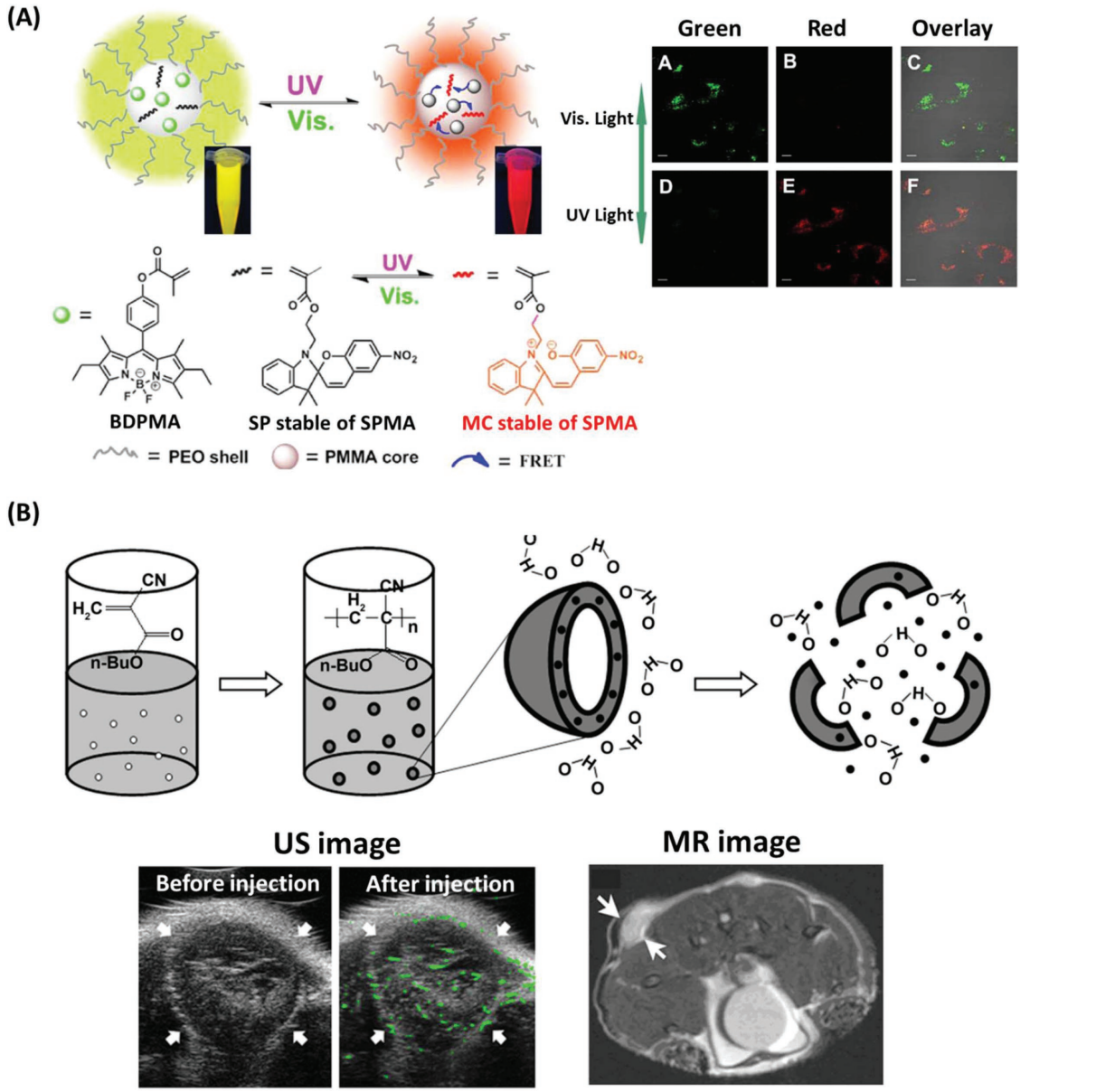

Figure 3. A) Schematic illustration of amphiphilic photoswitchable fluorescent polymeric nanoparticles (PFPNs) by covalently combining BODIPY monomer (BODIPY methacrylate, BDPMA) and photochromic derivative (spiropyran-linked methacrylate, SPMA) displaying reversibly distinct dual-color fluorescence via alternate illumination of UV and visible light. The SPMA adopted the ring-opened merocyanine (MC) state under UV irradiation, while changing to the ring-closed spiro (SP) state after visible light illumination. Confocal images of A549 cells treated with an amphiphilic PFPNs dispersion under visible light (inset A–C) or UV illumination (inset D–F). Scale bar: 10 µm. Modified with permission.[67] Copyright 2015, American Chemical Society. B) Schematic representation of the emulsion polymerization of butyl cyanoacrylate (BCA) and the O/W encapsulation of iron oxide nanoparticles in the bubble shell. Contrast-enhanced US images before and after magnetic hybrid microbubbles injection. T2-weighted MR image of tumor-bearing mouse after the injection of magnetic hybrid microbubbles. Modified with permission.[89] Copyright 2011, Elsevier.

that the γ-PGA/Cys@PANI nanogels could be used to generate heat in the tumor under laser irradiation, which was useful for photothermal therapy applications.

3.1.2. Magnetic Resonance Imaging

MRI is a medical technique with excellent soft tissue specificity based on nuclear magnetic resonance of the various interacting nuclei. T_1 (spin-lattice/longitudinal relaxation time), T_2 (transverse relaxation time), and ρ (spin energy) are the crucial values influencing MRI signal strengths.[74] Due to the difficulty to differentiate between normal tissues and tumors, contrast agents such as gadolinium complexes and magnetic nanoparticles were used to selectively highlight tumors. Gadolinium (Gd) complexes are promising contrast agents in MRI and can be encapsulated by miniemulsion polymerization.[75,76] However, in vivo transmetalation of Gd complexes with other metal ions

(copper, calcium, or zinc) can cause the release of free Gd, which increases the risk of nephrogenic systemic fibrosis and dermopathy.[77] Previous research reported the transmetalation of Gd complex with calcium ions.[78] Gd-DTPA-pullulan (gadolinium-diethylene triaminepentaaceticdianhydride-pullulan) was found to possess much higher stability than commercial Gd-EOB-DTPA (gadolinium-ethoxybenzyl-diethylenetriaminepentaacetic acid), suggesting a limitation of transmetalation. There are many attempts to improve the limitation of MRI in term of low sensitivity such as binding with noble metals (gold or silver) or conjugation with antibody.[79] Gold functionalized with gadolinium complexes was prepared by Moriggi et al.[80] Surface of gold nanoparticles (AuNPs) was functionalized with a thiol derivative of diethylenetriaminetetraacetic acid (DTTA) chelate. Thereafter, the resulting products were complexed with Gd (III) ions. The DTTA-functionalized AuNPs, which were complexed with Gd, yielded very high relaxivity. Besides Gd ions, magnetic nanoparticles are popular for targeted molecular imaging. Superparamagnetic iron oxide nanoparticles (SPIONs) are widely used as MRI contrast agents for cancer imaging.[81,82] With lower diffusivity of the SPIONs from the tumor, the SPIONs provided a longer time remaining in the tumor 24 h after injection, compared to 1 h for Gd-based contrast agents.[83] Polycaprolactone (PCL) encapsulated with magnetic nanoparticles was prepared by a double emulsion evaporation technique.[53] The prepared PCL/magnetic nanoparticles were compared with commercial Gadovist, which revealed that PCL/magnetic nanoparticles were suitable for T_2 contrast enhancement while commercial Gadovist was efficient for T_1-weighted images. Zhang and coworkers described the synthesis of uniform core–shell magnetic nanospheres with Fe_3O_4 as core and polystyrene/poly glycidyl methacrylate/lanthanide complex (gadolinium and Europium) as shell, by emulsifier-free emulsion polymerization.[22] These core–shell composites showed dual function of MRI and OI. In order to validate the feasibility of these core–shell composites as dual mode contrast agents for MR imaging, the core–shell composites were injected with a dose of 0.05 mmol Gd kg^{-1} of mouse. The presence of Fe_3O_4 nanoparticles and lanthanide complex exhibited high signal enhancement for both T_1 and T_2 MR signals in vitro and in vivo, and showed vivid red fluorescence luminescence in two-photon confocal scanning laser microscopy.

3.1.3. Positron Emission Tomography

PET is an attractive nuclear imaging technique based on the detection of photons arising from annihilation of electron (e^-) with a positron (e^+), emitted by PET radionuclide. PET can image deep tissue with high sensitivity (0.02–0.1 cps/Bq) and is widely used in preclinical and clinical imaging of diseases.[84] PET offers non-invasive quantification of biodistribution and concentration of probes labeled with radionuclides in a body and bloodstream such as determination of drug concentration in tissues as low as 10^{-12} mol L^{-1}.[85] Zhou et al. developed polymeric nanoparticles for brain penetration.[86] One way to treat glioblastoma multiforma (brain cancer) is to enhance the depth of penetration of locally delivered agents under a positive pressure gradient to create bulk fluid movement in the brain interstitium, called convection-enhanced delivery (CED). Therefore, PLGA nanoparticles prepared by emulsion-solvent evaporation technique were loaded with coumarin-6 (C6) and modified palmitoylated avidin to enable easy radiolabeling with *N*-(4-[^{18}F]fluorobenzyl)propanamido-PEG4-Biotin ([^{18}F]NPB4). The nanoparticles were injected and delivered via CED to right striatum of rats and pigs, and then observed by PET. The PET images showed that the mean volume of distribution (V_d) in the brain for the loaded PLGA nanoparticles was approximately 111 mm^3, whereas the mean V_d of standard PLGA nanoparticles (without loading and labeling) was approximately 53 mm^3. Thus, the brain-penetrating PLGA nanoparticles with loaded C6 and labeled [^{18}F]NPB4 could be delivered to large intracranial volumes in both rats and pigs.

3.1.4. Ultrasound Imaging

Ultrasound molecular imaging has emerged as promising non-invasive imaging method in biology and medicine. It has several advantages such as real-time practice, quantitative data, high temporal resolution, low cost, and non-ionizing radiation.[57] Ultrasound contrast agents can be divided into two groups: 1) gas-filled microbubble contrast agents and 2) non-microbubble contrast agents.[87] The gas-filled microbubble contains a gaseous core such as air, nitrogen, perfluorocarbon, or sulfur hexafluoride, surrounded by a shell typically of albumin, lipids, synthetic polymers, or galactose. Nonmicrobubble-based contrast agents, such as echogenic liposomes, perfluorocarbon nanodroplets, or solid nanoparticles, are submicron or nanosized particles.[88] Nonmicrobubble agents have advantages over microbubbles in term of efficiency to enter the extravascular space. Zhe Liu et al. designed multi-modal contrast agents for hybrid US and MRI imaging using iron oxide nanoparticle–embedded polymeric microbubbles.[89] Magnetic imaging probes were synthesized in a one-pot emulsion polymerization of butyl cyanoacrylate to form microbubbles with poly(butyl cyanoacrylate) shell, along with an oil-in-water (O/W) encapsulation of iron oxide nanoparticles in the bubble shell (Figure 3B). These magnetic imaging probes displayed a strong contrast in US and an increased transversal relaxation rate in MR. Moreover, the enhancing of longitudinal and transversal relaxivities was observed after destruction of US-induced bubbles.

3.1.5. Computed Tomography

CT is an X-ray technique that is widely used in medicine. CT has been developed to high resolution, called micro CT, to image organs or tissues. The main advantages of CT are high spatial resolution, fast acquisition time, relative simplicity, and excellent hard tissue imaging.[57,90] CT, however, is limited in discriminating between different soft tissues that have similar densities.[91] CT contrast agents were introduced to promote a contrast in soft tissue structure. Recently, many researches have focused on the development of nanoparticles as contrast agents. Nanoparticle contrast agents have advantages over small molecules (such as iodinated molecules) in term of long blood-pool residence time, and specific/targeted molecular

imaging. For instance, the circulation half-life of nanoparticles was 15 h, while that of iodinated small molecules was only minutes.[92] Patrick et al. have developed contrast agents based on nanoparticles containing iodine and poly(2-methacryloyloxyethyl (2,3,5-triiodobenzoate) (PMAOETIB), using microemulsion polymerization.[93] PMAOETIB consisted of non-soluble, iodine-carrying particles that circulated in the blood after being intravenously injected. Different surfactants such as cationic surfactants (cetyltrimethylammonium bromide and cetyltrimethylammonium chloride) and anionic surfactants (sodium oleate and sodium dodecyl sulfate) were used to control the particle size of these iodine-carrying nanoparticles which were ranging from 30 to 930 nm. The most favored surfactant for biocompatible application was sodium oleate. For medical application, PMAOETIB particles were injected into chicken thigh/lower leg (intramuscular), and CT images were recorded. PMAOETIB exhibited good CT contrast in chicken muscle.

3.2. Pharmacological Nanoparticles for Biosensing

Nanoparticles have been widely utilized as sensors of diseases, biological compounds, and toxic materials for diagnosis because they can detect analytes at very low concentrations.[94] Generally, the sensors are composed of two components that are a recognition element for target binding and a signal conversion unit.[1] Sensing detection of biological analytes such as DNA, RNA, proteins, or saccharides includes colorimetric, fluorescence, piezoelectric, and electrochemical measurements. Currently, nanoparticles are increasingly used for labeling and tracking cells in cell therapy. Real-time monitoring of cell status and functions was followed by reacting labeled nanoparticles with specific biomarkers. Yeo et al. have developed nanosensors of PLGA nanoparticles with encapsulated calcein acetomethoxy ester (CAM). Nanoparticle surface was functionalized with cationic poly(L-lysine) for an efficient endocytosis.[95] Generally, CAM is a weak fluorescent molecule, but it is converted into a strong fluorescent molecule in the presence of esterase. PLGA nanoparticles loaded with CAM were used to label and track mesenchymal stem cells (MSCs) to investigate cell viability. When the nanosensors were internalized in cells and released CAM was reacted with intracellular esterase, the fluorescence signal was turned "on," indicating cell viability. In the absence of esterase and even when the CAM molecules were released, the fluorescence was limited ("off"), as shown in **Figure 4**A. Practically, solution containing 2–10% dimethyl sulfoxide (DMSO) is known to be detrimental to cell health.[96] Thus, DMSO with various concentrations in the range of 0.01–2.5% v/v was treated to measure cell survival in the presence of PLGA nanoparticles loaded with CAM. As depicted in Figure 4A, cell survival can be observed from fluorescence signal, which was increased with decreasing DMSO concentration. Moreover, the confocal image also confirmed the distribution of these nanosensors located in an entire cytoplasm of MSCs. PLGA nanoparticles could be further used to monitor generation of nitric oxide in live cells because it plays a crucial role as secondary biochemical messenger in cardiovascular, physiological angiogenic, neurological, and immune systems.[97] In order to observe a strong fluorescence, 4-amino-5-methylamino-2′,7′-difluorescein diacetate (DAF-FM-DA) was encapsulated in PLGA nanoparticles. Similarly, in the presence of intracellular esterase, the released DAF-FM-DA was converted by deacetylation to 4-amino-5-methylamino-2′,7′-difluororescein (DAF-FM), which reacted with nitric oxide and yielded strong fluorescence. Human umbilical vein endothelial cells (HUVECs) were labeled with PLGA-loaded DAF-FM-DA nanosensors. The HUVECs responded to bradykinin peptide (Brady) by increasing calcium signaling that can trigger nitric oxide generation. However, the produced nitric oxide was inhibited by nitric oxide scavenger carboxy-PTIO (C-PTIO). Therefore, in the presence of Brady, the fluorescence signal of HUVECs labeled with PLGA nanosensors was the largest. When C-PTIO inhibitor was introduced, the fluorescence signal was at basal level, similar to a treatment of only nanosensor or Brady, as shown in Figure 4A. Therefore, these nanosensors can be utilized for bioimaging and biosensing.

3.3. Pharmacological Nanoparticles for Drug Delivery System

Nowadays, nanoparticles are frequently used for drug delivery systems. Nanoencapsulation of the drugs enhances their drug efficacy, target specificity, and tolerability.[100] Nanoencapsulation can also reduce the degradation of drugs and interaction of drugs with hazardous environment. Furthermore, the nanoparticles can improve the intracellular penetration.[50,101] Nanoparticles encapsulated with drugs (drug carriers) are superior to traditional drugs with respect to controlled release and targeted delivery.[102] Size, size distribution, and surface charge of drug carriers are important for the penetration of such carriers across the cell membrane. Drug delivery carriers are generally preferable to prepare solvent-free nanoparticles to avoid toxicity from solvents.[103] The drug carriers include liposomes, polymeric particles, core–shell particles, micelles, and dendrimers. Compared with solid nanoparticles, nanocapsules allow for encapsulation of large amount of drugs.[104] For example, thermo/pH-responsive targeted polymeric nanocapsules prepared from *N*-isopropylacrylamide, acrylic acid, and glycyrrhetic acid monomers for delivery of DOX were prepared by W/O/W double emulsion-solvent evaporation.[51] The glycyrrhetic acid was found to be a high affinity ligand for hepatic cancer. Therefore, the introduction of glycyrrhetic acid can improve the internalization of these nanocapsules into the hepatocyte via receptor-mediated endocytosis. Thermoresponsive polymers such as poly(*N*-isopropylacrylamide) was used as a temperature trigger for the release of anticancer drugs.[27] Polystyrene/poly(*N*-isopropylacrylamide) (PNIPAM)-silica core–shell nanoparticles with encapsulated 17-(allylamino)-17-demethoxygeldanamycin (17-AAG) were prepared by Pickering emulsion polymerization. Release of 17-AAG cancer drug from such core–shell nanoparticles was conducted at 40 and 25 °C. The release of 17-AAG at 40 °C was higher than that of room temperature due to shrinkage of the core–shell nanoparticles at temperature above the lower critical solution temperature of PNIPAM, resulting in drug release. Dalvi et al. designed the nanoparticles for targeted HIV reservoir by loading nevirapine in gold nanoparticles (AuNPs) using double emulsion-solvent evaporation.[52] AuNPs were mixed with DCM containing

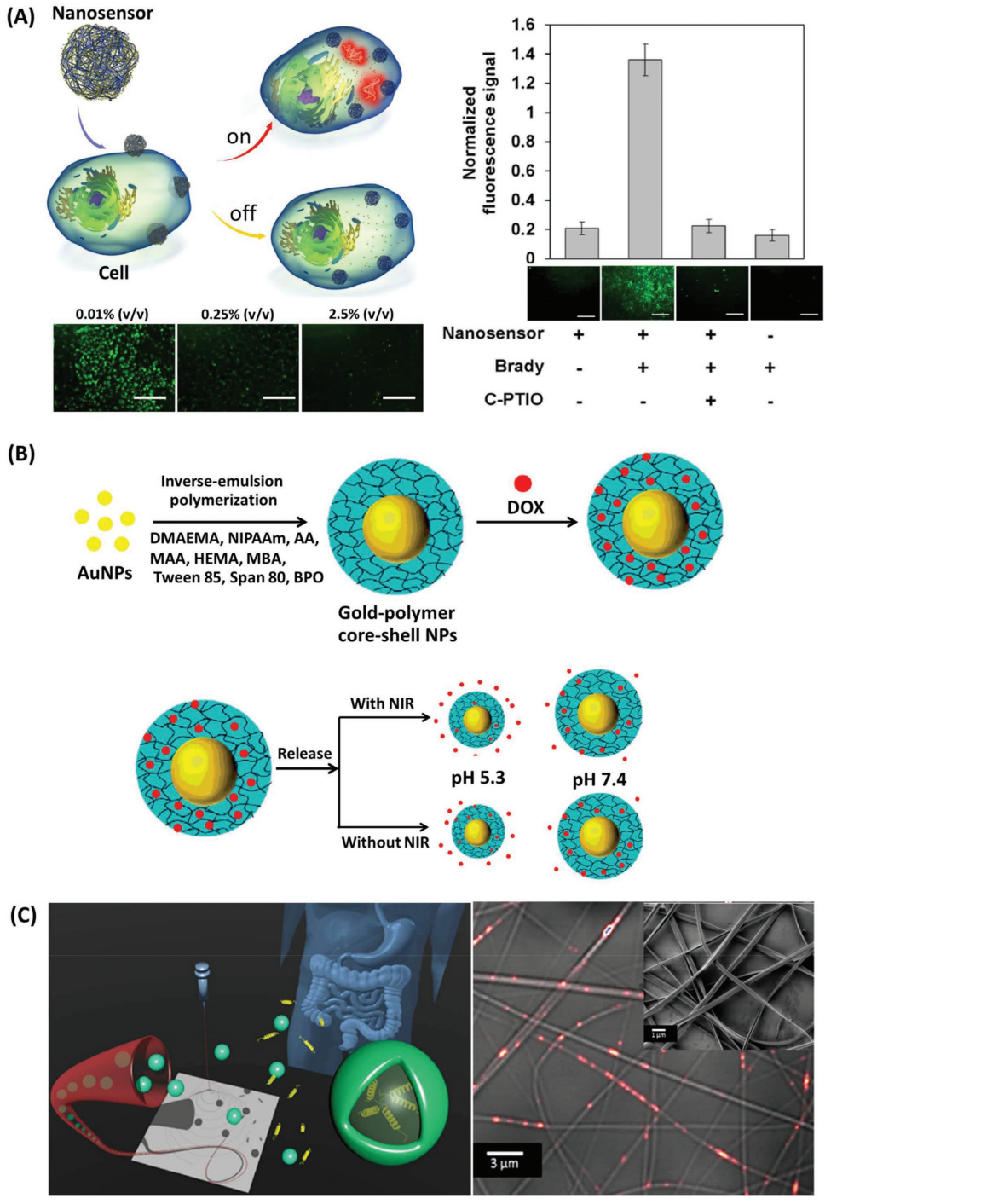

Figure 4. A) Schematic illustration of nanosensor platform in the presence/absence of biomarkers. Fluorescence images of PLGA-loaded CAM nanosensor–labeled mesenchymal stem cells (MSCs) at 24 h post-treatment with 0.01%, 0.25%, and 2.5% v/v DMSO. Fluorescence signal and images of PLGA-loaded 4-amino-5-methylamino-2′,7′-difluorescein diacetate (DAF-FM-DA) nanosensor–labeled human umbilical vein endothelial cells (HUVECs) in response to bradykinin (Brady) and nitric oxide scavenger carboxy-PTIO (C-PTIO). Scale bars represent 100 μm. Modified with permission.[95] Copyright 2015, Springer Nature. B) Fabrication process of gold-polymer core–shell nanoparticles used as DOX nanocarriers. Drug release profiles of gold-polymer core–shell nanoparticles loaded with DOX in the dark and under NIR. Modified with permission.[98] Copyright 2018, Elsevier. C) Schematic of the encapsulation polyelectrolyte complexes (PEC) nanoparticles in Eudragit L100-55 (EL55) fibers used in peptide delivery system (left); confocal image of EL55 nanofibers containing PEC nanoparticles (right); SEM image of EL55 nanofibers containing PEC nanoparticles (inset). Modified with permission.[106] Copyright 2017, American Chemical Society.

NVP, glyceryl monostearate (GMS), and dioctyl sulfosuccinate sodium salt (AOT). The primary emulsion was added in the aqueous surfactant solution to form core–shell nanoparticles. AuNPs loaded with NVP also showed rapid, high, and sustained accumulation in the possible HIV reservoir organs such as liver, spleen, lymph nodes, thymus, and remote locations of brain, ovary, and bone marrow. Moreover, AuNPs can also strongly absorb light irradiation energy and convert it to heat. Temperature can increase high enough to cause immediate cancerous cell death by disrupting their membranes.[105] Mahsa et al. demonstrated the effect of NIR light on the release of DOX from gold core–shell nanoparticles loaded with DOX with different pH values in dark room condition or under IR irradiation.[98] AuNPs were used as seeds in inverse emulsion polymerization of 2-(dimethylamino) ethylmethacrylate, *N*-isopropylacrylamide, acrylic acid, methacrylic acid, 2-hydroxyethyl methacrylate, and *N,N′*-methylenebis(acrylamide). As shown in Figure 4B, nanoparticles exhibited larger release at pH 5.3 than at pH 7.4 because of higher solubility of DOX in acidic media. Moreover, under NIR light, the drug can be more released from nanoparticles than in dark condition because AuNPs induced an increase of temperature of medium.

In the case of sensitive drugs such as peptides, drug carriers need to protect peptides from degradation. Previous research proposed a possible strategy for the preparation of drug carriers embedded in nanofibers.[106] Colloidal polyelectrolyte complexes (PECs) of polyglutamic acid, glycol chitosan, and rat peptide PYY were prepared by miniemulsion.[99] Encapsulation of PEC nanoparticles in Eudragit L100-55 (EL55) nanofibers was verified by confocal fluorescent microscopy (Figure 4C).[99] A sequence-controlled delivery of peptide was demonstrated, in which PEC nanoparticles were released from nanofibers and thereafter peptides were released from nanoparticles. From this strategy, the peptide payloads were not degraded before release because of protecting layers of nanofibers and nanoparticles.

4. Current Challenges and Opportunities in the Future

Evolution of pharmacological nanoparticles prepared by emulsion techniques has been marked by three aspects: 1) materials or reagents must be less toxic; 2) the formulations should have enough yield and drug encapsulation efficiency; and 3) the synthetic procedure should be reproducible and simple to allow economic scale-up.

The major problem of nanomaterials for in vivo imaging, biosensing, and drug delivery system is the potential long-term toxicity concern. Most nanomaterials after intravenous injection are accumulated by mononuclear phagocyte systems in organs such as liver, kidney, and spleen. Therefore, the selection of materials to use in human body is crucial. Another major challenge for the development of drug nanocarriers is that they shall deliver enough drug to targeted areas. Furthermore, most of the designed nanoparticles and techniques for nanoparticle fabrication are still confined to laboratory use. Large-scale fabrication, packaging, and shelf-life need to be addressed before being translated to clinical settings.

5. Conclusions

Nanoparticles fabricated by emulsion techniques have been proposed for drug delivery, biosensing, and bioimaging. Each emulsion technique offers different advantages such as ultralow interfacial tension for microemulsion, high encapsulation efficiency for double emulsion-solvent evaporation method, and fast preparations for emulsion polymerization. Nanoparticles can overcome limitations of conventional delivery methods such as specific targeting, specific tacking, strong fluorescence, insolubility, and instability of biomolecules. A wide variety of biomolecules was encapsulated or decorated on the nanoparticles both in the core and surface of nanoparticles. Monitoring and detection with nanoparticles in bioimaging are useful for early detection of disease and injury. Moreover, biosensor nanoparticles allow precise quantification at very low concentrations of analytes.

Acknowledgements

This work was supported by the postdoctoral fellowship from Vidyasirimedhi Institute of Science and Technology (VISTEC) and the Office of Higher Education Commission of Thailand (OHEC).

Conflict of Interest

The authors declare no conflict of interest.

Keywords

bioimaging, biosensor, drug delivery, emulsion, nanoparticles

Received: February 24, 2019
Revised: April 10, 2019
Published online:

[1] M. De, P. S. Ghosh, V. M. Rotello, *Adv. Mater.* **2008**, *20*, 4225.
[2] W. Jiang, B. Y. Kim, J. T. Rutka, W. C. Chan, *Nat. Nanotechnol.* **2008**, *3*, 145.
[3] H. Jahangirian, E. G. Lemraski, T. J. Webster, R. Rafiee-Moghaddam, Y. Abdollahi, *Int. J. Nanomed.* **2017**, *12*, 2957.
[4] J. Wang, X. Hu, D. Xiang, *Drug Deliv.* **2018**, *25*, 1319.
[5] F. Zhao, Y. Zhao, Y. Liu, X. Chang, C. Chen, Y. Zhao, *Small* **2011**, *7*, 1322.
[6] M. Beck-Broichsitter, I.E. Paulus, A. Greiner, T. Kissel, *Eur. J. Pharm. Biopharm.* **2015**, *92*, 96.
[7] S. A. Malik, W. H. Ng, J. Bowen, J. Tang, A. Gomez, A. J. Kenyon, R.M. Day, *J. Colloid Interface Sci.* **2016**, *467*, 220.
[8] H. Lee, S. An, S. Kim, B. Jeon, M. Kim, I. S. Kim, *Sci. Rep.* **2018**, *8*, 15725.
[9] T. F. Tadros, *Emulsion Formation and Stability*, John Wiley & Sons, New York **2013**.
[10] C. Sabliov, H. Chen, R. Yada, *Nanotechnology andFunctional Foods: Effective Delivery of Bioactive Ingredients*, John Wiley & Sons, New York **2015**.
[11] N. Pirooznia, S. Hasannia, A. S. Lotfi, M. Ghanei, *J. Nanobiotechnol.* **2012**, *10*, 20.

[12] S. Behzadi, M. Steinmann, D. Estupiñán, K. Landfester, D. Crespy, *J. Controlled Release* **2016**, *242*, 119.
[13] D.-m. Qi, Y.-z. Bao, Z.-x. Weng, Z-m. Huang, *Polymer* **2006**, *47*, 4622.
[14] R. Jenjob, F. Seidi, D. Crespy, *Adv. Colloid Interface Sci.* **2018**, *260*, 24.
[15] C. Chern, *Prog. Polym. Sci.* **2006**, *31*, 443.
[16] A. Kurozuka, S. Onishi, T. Nagano, K. Yamaguchi, T. Suzuki, H. Minami, *Langmuir* **2017**, *33*, 5814.
[17] S. C. Thickett, R. G. Gilbert, *Polymer* **2007**, *48*, 6965.
[18] C-S. Chern, *Principles and Applications of Emulsion Polymerization*, John Wiley & Sons, New York **2008**.
[19] H. B. Yamak, in *Polymer Science*, IntechOpen,London **2013**.
[20] J. Vanderhoff, E. Bradford, H. Tarkowski, J. Shaffer, R. Wiley, in *Polymerization and Polycondensation Processes* (Ed: N. A. J. Platzer), ACS Publications, Washington, DC **1962**.
[21] Y. Zhao, C. Shi, X. Yang, B. Shen, Y. Sun, Y. Chen, X. Xiaowei, S. Hongchen, Y. Kui, Y. Bai, L. Quan, *ACS Nano* **2016**, *10*, 5856.
[22] L. Zhang, S. Liang, R. Liu, T. Yuan, S. Zhang, Z. Xu, H. Xu, *Colloids Surf., B* **2016**, *144*, 344.
[23] S. H. Piao, S. H. Kwon, W. L. Zhang, H. J. Choi, *Soft Matter* **2015**, *11*, 646.
[24] Y. Yang, Z. Fang, X. Chen, W. Zhang, Y. Xie, Y. Chen, Z. Liu. W. Yuan, *Front. Pharmacol.* **2017**, *8*, 287.
[25] Y. Sun, T. Ren, Z. Deng, Y. Yang, S. Zhong, *New J. Chem.* **2018**, *42*, 7355.
[26] X. Pei, Y. Tan, K. Xu, C. Liu, C. Lu, P. Wang, *Polym. Chem.* **2016**, *7*, 3325.
[27] S. Sanyal, H. Huang, K. Rege, L. L. Dai, *J. Nanomedic. Nanotechnol.* **2011**, *2*, 126.
[28] D. Crespy, K. Landfester, *Beilstein J. Org. Chem.* **2010**, *6*, 1132.
[29] D. Schaeffel, R. H. Staff, H.-J. Butt, K. Landfester, D. Crespy, K. Koynov, *Nano Lett.* **2012**, *12*, 6012.
[30] D. Crespy, K. Landfester, *Soft Matter* **2011**, *7*, 11054.
[31] S. Behzadi, M. Gallei, J. Elbert, M. Appold, G. Glasser, K. Landfester, D. Crespy, *Polym. Chem.* **2016**, *7*, 3434.
[32] D. V. Amato, D. N. Amato, A. S. Flynt, D. L. Patton, *Polym. Chem.* **2015**, *6*, 5625.
[33] J.M. Asua, *Prog. Polym. Sci.* **2002**, *27*, 1283.
[34] R. Nagarajan, E. Ruckenstein, *Langmuir* **2000**, *16*, 6400.
[35] M. Hou, L. Dang, T. Liu, Y. Guo, Z. Wang, *ACS Appl. Mater. Interfaces* **2017**, *9*, 25747.
[36] W. Chen, X. Liu, Y. Liu, Y. Bang, H-I. Kim, *Colloids Surf. A* **2010**, *364*, 145.
[37] J. M. O'Donnell, *Chem. Soc. Rev.* **2012**, *41*, 3061.
[38] S. Liu, K. D. Hermanson, E. W. Kaler, *Macromolecules* **2006**, *39*, 4345.
[39] Â. S. Inácio, K. A. Mesquita, M. Baptista, J. Ramalho-Santos, W. L. Vaz, O. V. Vieira, *PLoS One.* **2011**, *6*, e19850.
[40] R. L. Grant, C. Yao, D. Gabaldon, D. Acosta, *Toxicology* **1992**, *76*, 153.
[41] W. Ming, F. N. Jones, S. Fu, *Polym. Bull.* **1998**, *40*, 749.
[42] S. C. Pilcher, W. T. Ford, *Macromolecules* **1998**, *31*, 3454.
[43] W. Ming, F. N. Jones, S. Fu, *Macromol. Chem. Phys.* **1998**, *199*, 1075.
[44] H. K. Yoon, A. Ray, Y-EK. Lee, G. Kim, X. Wang, R. Kopelman, *J. Mater. Chem. B* **2013**, *1*, 5611.
[45] R. H. Staff, K. Landfester, D. Crespy, in *Hierarchical Macromolecular Structures: 60 Years after the Staudinger Nobel Prize II*, Springer, Berlin **2013**.
[46] C. Bohlender, K. Landfester, D. Crespy, A. Schiller, *Part. Part. Syst. Charact.* **2013**, *30*, 138.
[47] S. Desgouilles, C. Vauthier, D. Bazile, J. Vacus, J-L. Grossiord, M. Veillard, C. Patrick, *Langmuir* **2003**, *19*, 9504.
[48] L.-Y. Guo, S.-Z. Yan, Q. Li, Q. Xu, X. Lin, S.-S. Qi, S.-Q. Yu, S.-L. Chen, *RSC Adv.* **2017**, *7*, 42073.
[49] M. Iqbal, N. Zafar, H. Fessi, A. Elaissari, *Int. J. Pharm.* **2015**, *496*, 173.
[50] J. Liu, Z. Qiu, S. Wang, L. Zhou, S. Zhang, *Biomed. Mater.* **2010**, *5*, 065002.
[51] X. He, F. Liang, F. Wang, L. Zou, J. Wang, C. Tang, K. Zhao, D. Wie, *J. Mater. Sci.* **2018**, *53*, 2326.
[52] B. R. Dalvi, E. A. Siddiqui, A. S. Syed, S. M. Velhal, A. Ahmad, A. B. Bandivdekar, P. V. Devarajan, *Curr. Drug Deliv.* **2016**, *13*, 1071.
[53] N. Ahmed, N. M. Ahmad, H. Fessi, A. Elaissari, *Colloids Surf., B* **2015**, *130*, 264.
[54] W. H. De Jong, P. J. Borm, *Int. J. Nanomed.* **2008**, *3*, 133.
[55] P. Sharma, S. Brown, G. Walter, S. Santra, B. Moudgil, *Adv. Colloid Interface Sci.* **2006**, *123-126*, 471.
[56] J. K. Willmann, N. Van Bruggen, L. M. Dinkelborg, S. S. Gambhir, *Nat. Rev. Drug Discovery* **2008**, *7*, 591.
[57] Z.-Y. Chen, Y.-X. Wang, Y. Lin, J.-S. Zhang, F. Yang, Q.-L. Zhou, Y.-Y. Liao, *Biomed Res. Int.* **2014**, *2014*, 819324.
[58] C. D. Bird, N. J. Emery, *Proc. Natl. Acad. Sci.* USA **2009**, *106*, 10370.
[59] A. Reisch, A. S. Klymchenko, *Small* **2016**, *12*, 1968.
[60] R. d. Sauer, A. Turshatov, S. Baluschev, K. Landfester. *Macromolecules* **2012**, *45*, 3787.
[61] C. Herrmann, A. Turshatov, D. Crespy, *ACS Macro Lett.*. **2012**, *1*, 907.
[62] O. Zupke, E. Distler, D. Baumann, D. Strand, R. Meyer, K. Landfester, W. Herr, V. Mailänder, *Biomaterials* **2010**, *31*, 7086.
[63] A. Monguzzi, M. Frigoli, C. Larpent, F. Meinardi, *RSC Adv.*. **2012**, *2*, 11731.
[64] X. Zhou, F. Su, H. Lu, P. Senechal-Willis, Y. Tian, R. H. Johnson, D. R. Meldrum, *Biomaterials.* **2012**, *33*, 171.
[65] J. Chen, Y. Tang, H. Wang, P. Zhang, Y. Li, J. Jiang, *J. Colloid Interface Sci.* **2016**, *484*, 298.
[66] M. Yu, P. Zhang, B. P. Krishnan, H. Wang, Y. Gao, S. Chen, R. Zeng, J. Cui, J. Chen, *Adv. Funct. Mater.* **2018**, *28*, 1804759.
[67] J. Chen, W. Zhong, Y. Tang, Z. Wu, Y. Li, P. Yi, J. Jiang, *Macromolecules* **2015**, *48*, 3500.
[68] L. Ge, Y. Tian, *Anal. Chem.* **2019**, *91*, 3294.
[69] S. Suarasan, A-M. Craciun, E. Licarete, M. Focsan, K. Magyari, S. Astilean, *ACS Appl. Mater. Interfaces* **2019**, *11*, 7812.
[70] T. Zhou, T. Luo, J. Song, J. Qu, *Anal. Chem.* **2018**, *90*, 2170.
[71] T. Shen, Y. Zhang, AM. Kirillov, B. Hu, C. Shan, W. Liu, Y. Tang, *J. Mater. Chem. B* **2016**, *4*, 7832.
[72] Q. Tang, W. Si, C. Huang, K. Ding, W. Huang, P. Chen, Q. Zhang, X. Dong, *J. Mater. Chem. B* **2017**, *5*, 1566.
[73] Y. Zhou, Y. Hu, W. Sun, B. Zhou, J. Zhu, C. Peng, M. Shen, X. Shi, *Nanoscale* **2017**, *9*, 12746.
[74] W. Wu, Z. Wu, T. Yu, C. Jiang, W.-S. Kim, *Sci. Technol. Adv. Mater.* **2015**, *16*, 023501.
[75] K. Malzahn, S. Ebert, I. Schlegel, O. Neudert, M. Wagner, G. Schütz, A. Ide, F. Roohi, K. Münnemann, D. Crespy, K. Landfester, *Adv. Healthcare Mater.* **2016**, *5*, 567.
[76] I. Schlegel, P. Renz, J. Simon, I. Lieberwirth, S. Pektor, N. Bausbacher, M. Miederer, V. Mailänder, R. Muñoz-Espí, D. Crespy, K. Landfester, *Macromol. Biosci.* **2018**, *18*, 1700387.
[77] W. P. Cacheris, S. C. Quay, S. M. Rocklage, *Mag. Reson. Imaging* **1990**, *8*, 467.
[78] R. Jenjob, N. Kun, J. Y. Ghee, Z. Shen, X. Wu, S. K. Cho, D. H. Lee, S. G. Yang, *Mater. Sci. Eng., C* **2016**, *61*, 659.
[79] J. Yang, C.-H. Lee, J. Park, S. Seo, E.-K. Lim, Y. J. Song, J.-S. Suh, H.-G. Yoon, Y.-M. Hu, S. Haam, *J. Mater. Chem.* **2007**, *17*, 2695.
[80] L. Moriggi, C. Cannizzo, E. Dumas, C. R. Mayer, A. Ulianov, L. Helm, *J. Am. Chem. Soc.* **2009**, *131*, 10828.

[81] H. Lee, E. Lee, D. K. Kim, N. K. Jang, Y. Y. Jeong, S. Jon, *J. Am. Chem. Soc.* **2006**, *128*, 7383.
[82] L. Li, W. Jiang, K. Luo, H. Song, F. Lan, Y. Wu, Z. Gu, *Theranostics* **2013**, *3*, 595.
[83] W. S. Enochs, G. Harsh, F. Hochberg, R. Weissleder, *J. Mag. Reson. Imaging* **1999**, *9*, 228.
[84] M. L. Fabiilli, M. R. Piert, R. A. Koeppe, P. S. Sherman, C. A. Quesada, O. D. Kripfgans, *Contrast Media Mol. Imaging* **2013**, *8*, 366.
[85] S. R. Cherry, *J. Clin. Pharmacol.* **2001**, *41*, 482.
[86] J. Zhou, T. R. Patel, R. W. Sirianni, G. Strohbehn, M-Q. Zheng, N. Duong, T. Schafbauer, A. J. Huttner, Y. Huang, R. E. Carson, Y. Zhang, D. J. Sullivan, J. M. Piepmeier, W. M Saltzman, *Proc. Natl. Acad. Sci.* USA **2013**, *110*, 11751.
[87] N. Deshpande, A. Needles, J. K. Willmann, *Clin. Radiol.* **2010**, *65*, 567.
[88] G. M. Lanza, S. A. Wickline, *Prog. Cardiovasc. Dis.* **2001**, *44*, 13.
[89] Z. Liu, T. Lammers, J. Ehling, S. Fokong, J. Bornemann, F. Kiessling, J. Gätjens, *Biomaterials* **2011**, *32*, 6155.
[90] D. P. Cormode, P. C. Naha, Z. A. Fayad, *Contrast Media Mol. Imaging* **2014**, *9*, 37.
[91] S.-B. Yu, A. D. Watson, *Chem. Rev.* **1999**, *99*, 2353.
[92] Q.-Y. Cai, S. H. Kim, K. S. Choi, S. Y. Kim, S. J. Byun, K. W. Kim, S. H. Park, S. K. Juhng, K. H. Yoon, *Invest. Radiol.* **2007**, *42*, 797.
[93] P. Illert, B. Wängler, C. Wängler, T. Röder, *Polym. Adv. Technol.* **2017**, *28*, 1610.
[94] E. C. Wang, A. Z. Wang, *Integr. Biol.* **2014**, *6*, 9.
[95] D. Yeo, C. Wiraja, Y. J. Chuah, Y. Gao, C. Xu, *Sci. Rep.* **2015**, *5*, 14768.
[96] J. Galvao, B. Davis, M. Tilley, E. Normando, M. R. Duchen, M. F. Cordeiro, *FASEB J.* **2014**, *28*, 1317.
[97] J. Xu, W. Wang, M. Ludeman, K. Cheng, T. Hayami, J. C. Lotz, S. Kapila, *Tissue Eng., Part A* **2008**, *14*, 667.
[98] M. Mazloomi-Rezvani, M. Salami-Kalajahi, H. Roghani-Mamaqani, *Colloids Surf., B* **2018**, *166*, 144.
[99] W. He, M. Parowatkin, V. Mailänder, M. Flechtner-Mors, R. Graf, A. Best, K. Koynov, K. Mohr, U. Ziener, K. Landfester, D. Crespy, *Biomacromolecules* **2015**, *16*, 2282.
[100] U. Schroeder, P. Sommerfeld, S. Ulrich, B. A. Sabel, *J. Pharm. Sci.* **1998**, *87*, 1305.
[101] F. Alexis, E. Pridgen, L. K. Molnar, O. C. Farokhzad, *Mol. Pharmaceutics* **2008**, *5*, 505.
[102] A. Kumari, S. K. Yadav, S. C. Yadav, *Colloids Surf., B* **2010**, *75*, 1.
[103] M. Esfandyari-Manesh, M. Javanbakht, R. Dinarvand, F. Atyabi, *J. Mater. Sci.: Mater. Med.* **2012**, *23*, 963.
[104] Y. Zhao, L.-P. Lv, S. Jiang, K. Landfester, D. Crespy, *Polym. Chem.* **2015**, *6*, 4197.
[105] W. Cai, F. Chen. *Hybrid Nanomaterials: Design, Synthesis, and Biomedical Applications*, CRC Press, Boca Raton, FL **2017**.
[106] C.W. He, M. Parowatkin, V. Mailänder, M. Flechtner-Mors, U. Ziener, K. Landfester, D. Crespy, *ACS Appl. Mater. Interfaces* **2017**, *9*, 3885.